CHEMISTRY
A EUROPEAN JOURNAL

DOI: 10.1002/chem.201001288

A Piggyback Ride for Transition Metals: Encapsulation of Exohedral Metallofullerenes in Carbon Nanotubes

Thomas W. Chamberlain, Neil R. Champness, Martin Schröder, and Andrei N. Khlobystov*[a]

Abstract: We have developed a method that enables the efficient insertion of transition-metal atoms and their small clusters into carbon nanotubes. As a model system, Os complexes attached to the exterior of fullerene C_{60} (exohedral metallofullerenes) were shown to be dragged into the nanotube spontaneously and irreversibly due to strong van der Waals interactions, specific to fullerenes and carbon nanotubes. The size of the metal-containing groups attached to C_{60} was shown to be critical for successful insertion, as functional groups too bulky to enter the nanotube were stripped off the fullerene during the encapsulation process. Once inside the nanotube, Os atoms catalyse polymerisation and decomposition of fullerene cages, which is related to a much higher catalytic activity of metal atoms situated on the surface of the fullerene cage, as compared to metal atoms in endohedral fullerenes, such as $M@C_{82}$. Thus, exohedral metallofullerenes show promise for applications in catalysis in carbon "nano" test tubes.

Keywords: fullerenes · nanotubes · noncovalent interactions · transition metals · transmission electron microscopy

Introduction

Owing to their extremely high mechanical stability, relative chemical inertness, and the availability of different diameters from sub-nanometre to hundreds of nanometres, carbon nanotubes have been widely used as nano-sized containers for molecules and atoms.[1] Molecules and atoms encapsulated in nanotubes are often arranged in geometrically regular, 1D arrays, some of which do not exist outside carbon nanotubes and thus can be regarded as products of confinement at the nanoscale.[1] The structural and dynamic properties of some materials encapsulated in nanotubes change drastically as a result of this confinement, and there is a growing body of evidence that the chemical reactivity of encapsulated compounds can also be altered inside carbon nanotubes.[2]

In turn, the physicochemical properties of nanotubes can be significantly affected by the species present inside, and this offers a methodology for tuning the functional properties of nanotubes, such as the electronic band gap, and the concentration and mobility of charge carriers.[2] Transition metal[3] and lanthanide[4,5] containing molecules appear to be most effective for this purpose as the metal atoms encapsulated in nanotubes provide magnetically, optically, redox or catalytically active centres within the nanotube structure.

The presence of well-defined metal centres within carbon nanotubes is highly desirable, but the methods of insertion of metals in nanotubes are still far from perfect. Insertion of liquid metals in nanotubes is prohibitive because of their high surface tension, whereas insertion of molten metal salts, which also relies upon capillary forces, is cumbersome because of the high melting temperature of most transition-metal salts. As a result, neither of these methods produces nanotubes efficiently filled with well-defined, metal-containing species.

The most efficient method of insertion of metals into nanotubes relies on specific non-covalent interactions between the nanotube and the guest species. Endohedral metallofullerenes—$M@C_n$ (Figure 1a)—in which a single metal atom or a small cluster of metal atoms are incarcerated in a cage of n carbon atoms, are strongly attracted to the internal cavity of the nanotube due to the highly effective van der Waals interactions between the surface of the endohedral fullerene and the nanotube interior. The fullerene–nanotube interaction energy has been measured to be ≈ 3.0 eV

[a] Dr. T. W. Chamberlain, Prof. N. R. Champness, Prof. M. Schröder, Dr. A. N. Khlobystov
School of Chemistry, University of Nottingham
Nottingham, NG7 2RD (UK)
Fax: (+44) 115-951-3563
E-mail: andrei.khlobystov@nottingham.ac.uk

Supporting information for this article is available on the WWW under http://dx.doi.org/10.1002/chem.201001288.

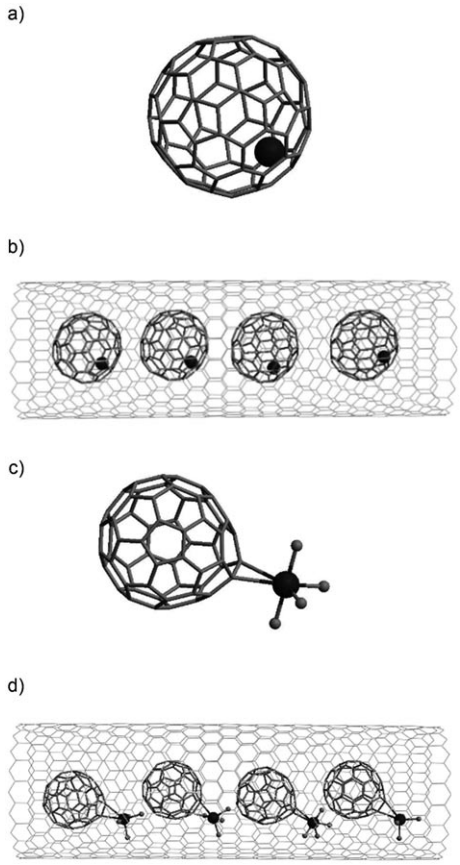

Figure 1. a) Endohedral metallofullerene, b) endohedral metallofullerenes encapsulated in a SWNT, c) exohedral metallofullerene, d) exohedral metallofullerenes encapsulated in SWNT.

(288 kJ mol^{-1}) for C_{60} and a single-walled carbon nanotube (SWNT),[6] and can be higher for larger fullerene cages. Previously, we[5,7,8] and others[9,10] have exploited the unique affinity of nanotubes to absorb fullerenes with metals inside leading to (M@C_n)@SWNT structures in an exceptionally high yield (up to 100%), in which metal atoms are arranged in a perfect chain along the nanotube channel (Figure 1b).

One of the problems with the use of endohedral fullerenes is that preparation of these molecules requires highly specialised equipment (electric arc-discharge) and extensive HPLC purification with a typical overall yield of less than 1%. As a result, endohedral fullerenes are only available in small quantities in a handful of laboratories round the world. Another disadvantage of endohedral fullerenes is that the range of metals available for this approach is typically restricted to the Group III elements, with very few examples of transition-metal-containing endohedral fullerenes reported.[11] The final issue is related to the fact that the metal atom is fully encased within the fullerene cage, and is, therefore, not directly accessible for electronic interactions with the nanotube sidewalls or catalytic reactions with other guest molecules. Although it has been demonstrated that once endohedral fullerenes are inside the nanotube, it is possible to break the fullerene cages by heating (1300–1400°C)[12,13] or using radiation,[8,9] thereby liberating the metal atoms into the nanotube cavity, these are often high-energy processes and difficult to control.

We report herein an alternative strategy for encapsulation of metal atoms in carbon nanotubes. We exploit the ability of fullerenes to act as an efficient ligand for many transition metals, leading to the formation of fullerene–metal complexes in which the metal is attached to the fullerene cage exohedrally (i.e., the outside of the cage, Figure 1c). We demonstrate that the fullerene cage bearing an exohedral metal atom or a cluster of atoms provides attractive interactions with the nanotube interior that are sufficiently strong to pull metal atoms into nanotubes (Figure 1d). Unlike the endohedral fullerene approach, which is currently restricted mostly to lanthanides, the use of fullerenes functionalised exohedrally with metal atoms enables the insertion of virtually any metal atom in the Periodic Table into nanotubes. Thus, our new approach provides a versatile, accessible and scalable alternative to the endohedral fullerenes.

Results and Discussion

Organometallic Os fullerene complexes **1** and **2** (Figure 2)[14] were chosen as model compounds to demonstrate the principle of transport and encapsulation of transition metals in nanotubes utilising exohedral metallofullerenes.

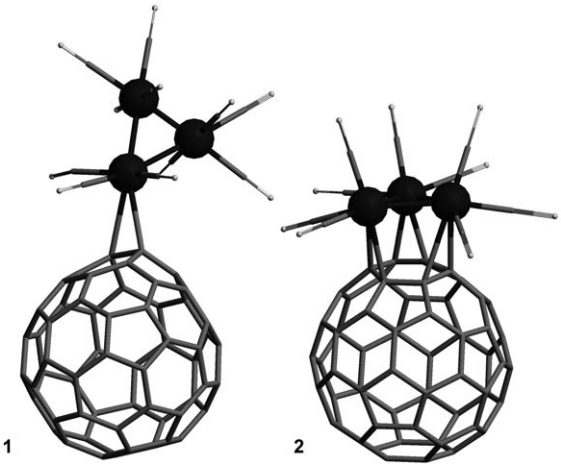

Figure 2. Exohedral metallofullerenes $[Os_3(CO)_{11}(\eta^2\text{-}C_{60})]$ (**1**) and $[Os_3(CO)_9(\mu_3\text{-}\eta^2,\eta^2,\eta^2\text{-}C_{60})]$ (**2**).

Complexes of Os have been reported as both promising hetero- and homogeneous catalysts[15] and are known to form carbides with interesting magnetic properties when treated at high temperatures.[16] Freshly opened SWNTs, prepared by arc discharge (NanoCarbLab) were immersed in a supersaturated solution of the exohedral metallofullerene dissolved in an organic solvent, following solution-based filling techniques recently developed for fullerenes.[17] A filling yield of between 15–20% has been estimated through

statistical transmission electron microscopy (TEM) analysis. Our previous extensive studies[18–20] show that the filling yield with functionalised fullerenes rarely exceeds 30%, and therefore yields observed in this study are considered to be relatively high. In contrast, under the same conditions unfunctionalised, pristine C_{60} can be inserted in nanotubes much faster and in a higher yield (up to 70%) than any functionalised fullerene.[21] Functional groups attached to C_{60} create a steric barrier for encapsulation if the fullerene axis is not aligned with the nanotube axis, and hinder the surface diffusion of fullerene molecules adsorbed on the nanotube, which is a vital stage in the nanotube filling mechanism.[1d] Although no comparative kinetic data for insertion of C_{60} and functionalised fullerenes is available at the moment, the lower filling yields consistently observed for functionalised species clearly suggest that the chemical functionality may create both thermodynamic and kinetic barriers. We are currently investigating the dynamics of fullerene transport and encapsulation by theoretical methods.

The filled nanotubes were imaged by using high-resolution TEM (HRTEM)—the only method that allows direct confirmation of the insertion of molecules and the presence of individual metal atoms or metal clusters within the SWNTs. Because TEM is an invasive characterisation technique that requires passing a beam of accelerated electrons (e-beam) through a specimen, the imaging conditions were set to minimise knock-on damage commonly observed for molecular structures by reducing the accelerating voltage to 100 kV and using the lowest possible current density of the e-beam on specimen. Imaging of C_{60}@SWNT under these conditions showed no structural changes in the fullerene molecules over 10–20 min, which confirms that any structural transformations of the exohedral metallofullerenes inside the nanotubes observed in this study are catalysed by Os metal atoms.

In our earlier studies,[19] we pioneered TEM imaging of fullerenes functionalised with organic groups susceptible to knock-on damage, and in this study we show that visualisation of intact organometallic molecules (i.e., exohedral metallofullerenes) is significantly more challenging because of their higher reactivity under the e-beam. Large field of view images (Figure 3a, b) that require only moderate e-beam current density, allow us to visualise clearly intact fullerene cages inside nanotubes for compounds **1** and **2** encapsulated within the SWNT, thus confirming that exohedral metallofullerenes are absorbed by carbon nanotubes from solution (Figure 3; see also Figure S1 in the Supporting Information). Although the direct visualisation of the exohedral functional groups attached to fullerenes is often problematic, the circular shape of the C_{60} cage can be clearly identified in large field of view micrographs,[18] which enables measurements and analysis of interfullerene separations for individual pairs of molecules.

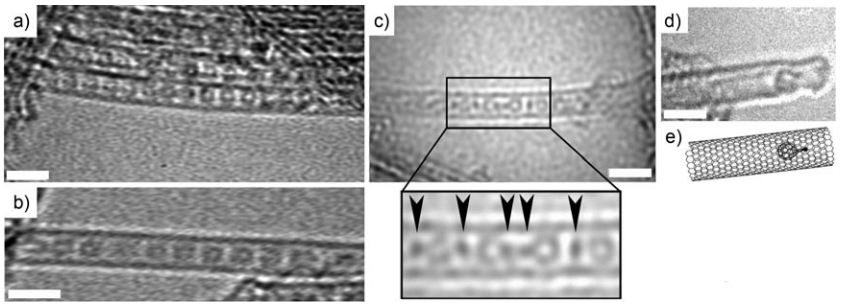

Figure 3. a), b) Large field of view HRTEM images of **1**@SWNT showing extended ordered arrays of exohedral metallofullerenes in SWNTs, c) high-magnification HRTEM image of **2**@SWNT with periodic high-contrast features (labelled with arrows in the enlarged region) corresponding to metal clusters spaced by fullerene cages. d) In **2**@SWNT the molecular motion is slowed down by interactions of the exohedral fullerene with defects in the nanotube sidewall, so that both the fullerene cage and the metal-containing group attached to it can be clearly observed. e) Molecular diagram showing the orientation of an exohedral metallofullerene in a SWNT (nanotube sidewall defects are not shown). Scale bars = 20 Å.

The average interfullerene spacing was measured for the two exohedral metallofullerenes **1** and **2** and a control sample of C_{60}@SWNT filled under identical conditions (Table 1). The mean interfullerene separation distance increases for each functionalised fullerene when compared to pristine C_{60} by a significant margin of 4.1–5.1 Å, indicating that the metal atoms are present in the interfullerene regions of the structure in the SWNT. As expected, exohedral fullerenes form less ordered molecular chains than pristine C_{60}, as indicated by the higher standard deviations for **1** and **2**@SWNT, which arises from the three orientations that the unsymmetrical molecules can adopt within the nanotube with relation to neighbouring fullerenes (head-to-head, head-to-tail, and tail-to-tail) and has been observed previously for functionalised fullerenes within SWNTs.[18]

Table 1. Geometrical parameters of C_{60}@SWNT, **1**@SWNT and **2**@SWNT structures as measured by HRTEM. Interfullerene separations are measured from centre-to-centre of fullerene cages for pairs of neighbouring molecules.

	Mean separation distance determined by HRTEM [Å]	Increase in separation [Å]	Standard deviation [Å]
C_{60}@SWNT	9.8	–	0.1
1@SWNT	13.9	4.1	1.4
2@SWNT	14.9	5.1	1.7

Imaging at high magnification provides direct evidence of metal atoms present within nanotubes for the sample **2**@SWNT (Figure 3c). However, the higher e-beam current density required for the high magnification images causes detachment of metal atoms from the fullerene and rapid damage of the carbon cages as shown in the time series of

HRTEM images obtained for **2**@SWNT (Figure 4). HRTEM contrast depends on the atomic number of elements as $\sqrt{Z}$, and so all of the dark contrast features observed inside nanotubes can be attributed to Os metal atoms ($Z=76$), as all the remaining elements in these materials are significantly lighter than osmium ($Z=6$ for carbon, and $Z=8$ for oxygen). The nature of the dark contrast features was verified by energy-dispersive X-ray (EDX) spectroscopy performed on individual nanotubes and nanotube bundles filled with compounds **1** and **2**. The EDX measurements confirm the identity of high-contrast atoms in nanotubes as osmium atoms (major EDX lines of Os are marked with arrows, Figure 5, see also Figure S1 in Supporting Information). The percentage of Os can be estimated as 0.25 ± 0.15 atomic% by taking EDX spectra of bundles of **1**@SWNT and **2**@SWNT, typically consisting of 50–100 nanotubes, with a highly focused e-beam matching the diameter of the bundle, which avoids the supporting carbon film.

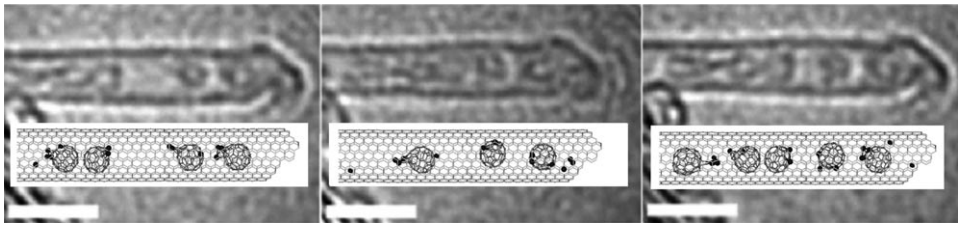

Figure 4. Time series (left to right) of HRTEM images of **2**@SWNT demonstrating rapid molecular motion and dissociation of Os–C bonds under the e-beam, scale bars = 20 Å.

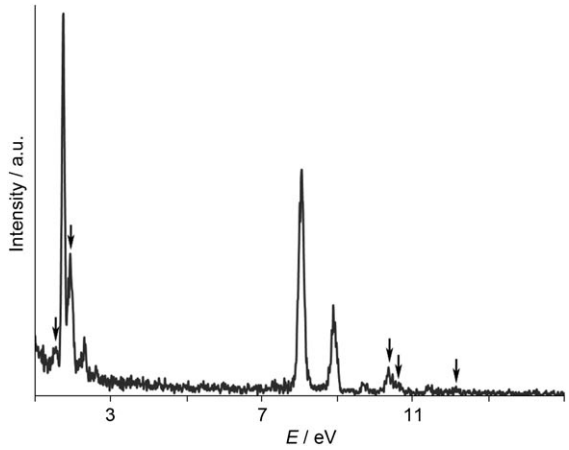

Figure 5. EDX spectrum taken for a bundle of **2**@SWNT (containing approximately 80 nanotubes). The major peaks of Os are marked with arrows. Other peaks are due to carbon and copper (material of the TEM electron gun assembly).

From structural considerations, an ideal nanotube completely filled with Os–fullerene complexes **1** or **2** (filling rate 100%) would have three atoms of osmium for approximately 280–360 atoms of carbon from the carbon nanotube (depending on the exact nanotube diameter) and 60 atoms of carbon of the fullerene cage. Therefore, the maximum possible atomic percentage of Os in structures **1**@SWNT and **2**@SWNT is about 0.7% against 99.3% of carbon. Comparing this with the experimental EDX measurements, the filling rate of nanotubes with the molecules can be estimated to be in the range of 35 ± 15%, which is consistent with the direct-space observations.

A series of images of the same nanotube filled with exohedral fullerene **2** obtained over a period of approximately 20 s (Figure 6) further illustrates the dynamic nature of the organometallic molecules under the e-beam. The e-beam current density was deliberately reduced in this series to prolong the life-time of the molecules, at the expense of image contrast. At the beginning of the series a chain of five intact metallofullerene molecules are seen in the middle part of the nanotube (each marked with a white arrowhead; Figure 6, top) oriented in a head-to-tail fashion. However, after a few seconds of irradiation with the e-beam the molecules start polymerisation and coalescence into an internal nanotube (Figure 6, bottom) with Os atoms seen to be

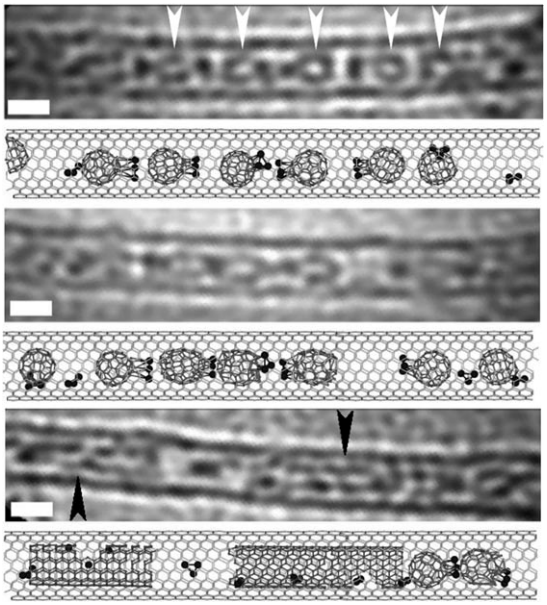

Figure 6. Time-sequence of HRTEM images and structural diagrams of the evolution of exohedral metallofullerene **2** in nanotubes. White arrows indicate the positions of five intact metallofullerene molecules with metal atoms to the side of each C_{60} cage (top image), and black arrows indicate segments of internal carbon nanotube formed through decomposition of **2**. Unfunctionalised fullerenes C_{60} (without Os-atoms) remain stable and do not decompose under these imaging conditions (100 kV, low current density), scale bars = 10 Å.

trapped within the interior walls of the resultant double-walled nanotube (DWNT, see also Figure S6 in the Supporting Information). Under the same conditions, pristine fullerenes (e.g., C_{60} and C_{70}) and endohedral metallofullerenes (e.g., $M@C_{82}$ and $M_3N@C_{80}$) remain intact inside nanotubes for significantly longer periods of time (up to 20 min). The fact that the exohedral metallofullerenes exhibit a significantly greater reactivity in nanotubes than other types of fullerenes is related to the high catalytic activity of transition metal (Os) that is situated on the surface of the fullerene cage, and therefore is readily accessible for chemical reactions within the carbon "nano" test tube. The chemical reactivity of metal atoms in endohedral fullerenes, such as $M@C_{82}$, is passivated by the fullerene shell enveloping that metal, so that the metal atom has to break through the shell in order to be involved in any chemical reactions within the nanotube.[8] This clearly requires significantly greater activation energy than in the present case of the exohedral metallofullerene.

Although many fullerene cages are observed for **1**@SWNT, a relatively small number of high contrast features corresponding to Os atoms were found for this compound. This could be due to the rapid rotation of the fullerene cage or the flexibility of the exohedral groups allowing the Os atoms to adopt more than one position within the time frame of the TEM image capture ($\approx$1 s). In complex **1** the Os_3 cluster is attached to C_{60} cage through only one metal atom, which makes it significantly more conformationally flexible compared to the Os_3 cluster in **2**. A similar phenomenon has been reported for $Sm@C_{82}$ in SWNTs, in which the fullerene cage exhibits a relatively fast continuous rotation inside the nanotube so that the Sm atoms were not visible in HRTEM until the fullerene cages eventually became immobile as a result of electron beam damage.[22,23] A small number of large dark contrast features were observed for **1**@SWNT that may result from Os-metal-atom-clustering induced by the electron beam (Figure 7 and Figures S2–S4 in the Supporting Information). In compound **2**, all three Os atoms are bonded to the fullerene cage, which restrains the metal cluster from rotating and allows the exohedral functionality to be visualised more clearly than for **1**, particularly when the molecule is temporary immobilised by the interactions with defects in nanotube sidewalls (Figure 3d).

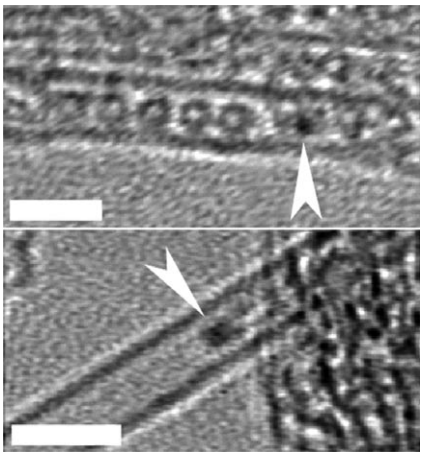

Figure 7. HRTEM images of **1**@SWNT with a high contrast features corresponding to Os-metal clusters (white arrow), scale bar = 20 Å.

The introduction of metal atoms into the internal cavity of nanotubes through either endohedral fullerene or metallocene encapsulation has been shown to have a dramatic effect on the electronic properties of SWNTs.[24,3] As electron acceptors, nanotubes will readily accept electrons from the metal species, leading to an increase in the number of charge carriers in the conduction band of the nanotube. This effect on addition of exohedrally coordinated osmium is likely to be greater than that of the protected endohedral metallofullerenes, as the metal, being outside the carbon cage in the former case, is more accessible for interactions with the carbon nanotube sidewalls. However, the oxidation potential of Os^0 is lower than that of cobaltocene, which makes the osmium–fullerene complexes more selective electron donors than the metallocene molecules. The doping effects of the exohedral metallofullerenes on carbon nanotubes is currently under investigation by Raman and photoluminescence (PL) spectroscopy and electron-transport measurements.

The effectiveness of the molecular encapsulation in nanotubes depends critically on the ratio of the nanotube diameter to the critical dimension of the guest molecule.[25] In order to probe the size selectivity of exohedral metallofullerene encapsulation in nanotubes, an Os fullerene derivative **3**[26] (Figure 8) was selected with a critical diameter of 15 Å that is comparable to the internal diameter of the SWNTs (14–15 Å) used in our experiments. After the nanotubes were immersed in a solution of **3**, HRTEM show C_{60} present in nanotubes in abundance, but with no evidence of any functional groups attached to the fullerene (Figure 8b). The interfullerene separation in this structure has been measured to be 9.89 ± 0.02 Å, which is virtually identical to C_{60}@SWNT assembled from pristine C_{60} and is significantly lower than that for any functionalised fullerenes in SWNTs.

These observations are explained by the fact that the fullerene cage of **3** is pulled into the SWNT with substantial energy (288 kJ mol^{-1}),[6] whereas the bulky functional group is physically unable to enter the nanotube (Figure 9b). Since the energy gain for encapsulation of the fullerene part of the molecule is significantly greater than the energy of the Os–fullerene bond (ca. 150 kJ mol^{-1})[27] decomposition of the complex is likely to occur with the fullerene cage entering the nanotube and Os metal fragment left outside (Figure 9c). This provides an explanation for the C_{60}@SWNT structures observed in this sample (Figure 8b). After Os atoms have been removed from the surface of fullerenes, the fullerene cages remain unchanged even after prolonged exposures to the e-beam, which confirms that no Os is present in the nanotubes.

The sterically bulky, Os-containing fragment detached from C_{60} will drift away from the nanotube and is likely to

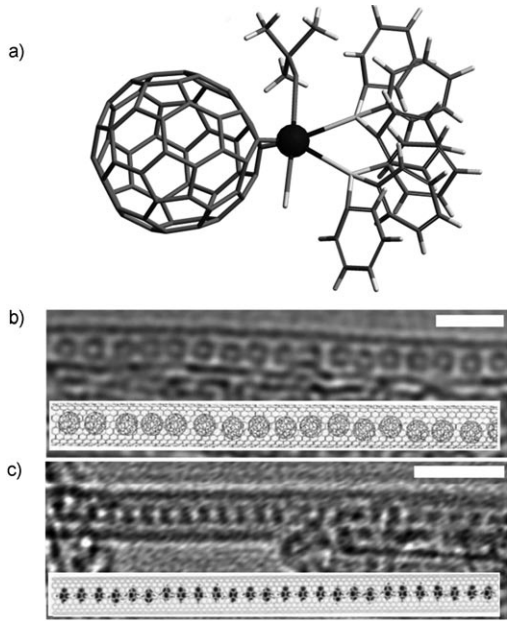

Figure 8. View of a) sterically bulky exohedral metallofullerene [Os-$(PPh_3)_2$*t*BuNC(CO)C_{60}] (**3**); b) HRTEM image and structural diagram showing C_{60} in nanotubes after treating the SWNT sample with a solution of exohedral metallofullerene **3**. Interfullerene separation is 9.89 ± 0.02 Å; c) HRTEM image and a structural diagram showing a chain of metal atoms in a narrow nanotube (the nanotube diameter is 10 Å, scale bars = 20 Å).

form an Os_2 dimer to satisfy the coordination requirement of the metal centres. Such a dimer is expected to be highly sterically crowded, and so it will lose the bulky ligands (e.g., Ph_3P, *t*BuNC) and regroup into a more compact molecule. Indeed, we observe that some narrow SWNTs (nanotube diameters 12.0–13.5 Å) are filled with metal-containing species arranged in a periodic fashion (Figure 8c).

The insertion of exohedral metallofullerenes in SWNT appears to be a spontaneous and irreversible process requiring only small activation energy. We have demonstrated that transition metals can be efficiently transported into nanotubes under very mild conditions using this approach. The surprisingly high reactivity of fullerene cages observed under the e-beam is a result of catalytic action of Os atoms. This study shows promise for such metal complexes encapsulated inside SWNTs to act as catalytically active centres for initiating chemical reactions in nanotubes and leading to the formation of new products inaccessible by other means. Encapsulation of optically or magnetically active fullerene–metal complexes will result in the formation of chains of molecules whose functional properties could be exploited in nanoelectronics devices.

Experimental Section

Single-walled carbon nanotubes were purchased from NanoCarbLab (arc discharge, 80% purity), C_{60} fullerene from SES Research (99% purity) and all other reagents from Sigma–Aldrich and used without further purification. Compounds **1**, **2** and **3** were prepared and isolated following reported methods,[14,26] and their composition and purity were verified by ^1H and ^{13}C NMR, IR spectroscopy and mass spectrometry (MALDI ToF ionisation mode), which were in agreement with the corresponding literature data.

Fullerenes **1** and **2** were inserted into nanotubes using the following general method. Purified nanotubes were annealed in air at 520 °C for 15 minutes. A threefold excess of fullerene was dispersed in $CHCl_3$ (1 mL) using an ultrasonic bath to form a super-saturated solution, which was added dropwise to the freshly annealed nanotubes in an agate mortar, allowing each drop to evaporate before adding a further drop. The resultant black solid was allowed to dry thoroughly in air, ground using a pestle and mortar for 5 min before being washed with carbon disulphide (20 mL) to remove any unencapsulated fullerenes and then with methanol (20 mL). Our recent study[17] has demonstrated that under this conditions fullerene molecules form large clusters, up to several million of molecules, which interact with nanotubes and exclude any detrimental influence of the solvent.

Approximately 0.5 mg of each sample was dispersed in methanol (2 mL) using an ultrasonic bath and the resultant suspensions were drop cast onto amorphous carbon-coated copper TEM grids. Each sample was imaged using JEOL-2100F TEM at 100 kV accelerating voltage.

Acknowledgements

This work was supported by the EPSRC, Nottingham Nanoscience and Nanotechnology Centre, European Science Foundation and the Royal Society. M.S. gratefully acknowledges receipt of a Royal Society Wolfson Merit award and of an ERC Advanced Grant.

[1] a) B. W. Smith, M. Monthioux, D. E. Luzzi, *Nature* **1998**, *396*, 323–324; b) S. Berber, Y.-K. Kwon, D. Tomanek, *Phys. Rev. Lett.* **2000**, *84*, 4613–4616; c) M. Yoon, S. Berber, D. Tomanek, *Phys. Rev. B* **2005**, *71*, 155406/1–4; d) H. Ulbricht, G. Moos, T. Hertel, *Phys. Rev. Lett.* **2003**, *90*, 095501/1–4; e) M. Hodak, L. A. Girifalco, *Phys. Rev. B* **2001**, *64*, 035407/1–9; f) A. N. Khlobystov, D. A. Britz, G. A. D. Briggs, *Acc. Chem. Res.* **2005**, *38*, 901–909.

[2] a) *Chemistry of Carbon Nanotubes* (Eds.: V. A. Basiuk, E. V. Basiuk), American Scientific, New York, **2008**; b) T. Lu, E. M. Gold-

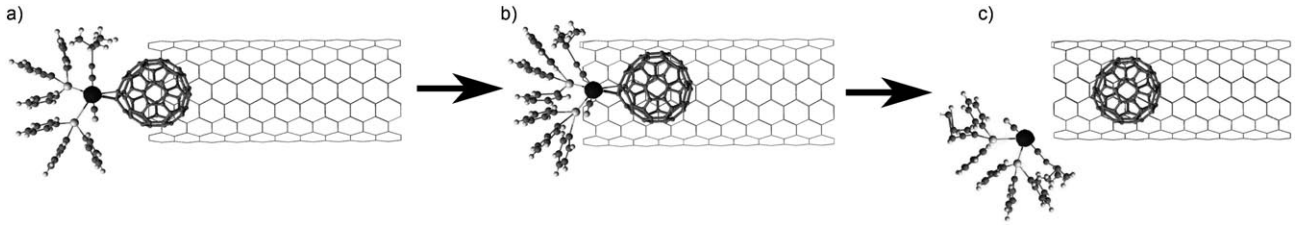

Figure 9. Sequential encapsulation and the subsequent decomposition of **3** in SWNT, showing how the organometallic functional group is forced to dissociate from the fullerene cage (c) as the fullerene moves progressively further into the SWNT during encapsulation ($d_{NT} = 14$–15 Å).

field, S. K. Gray, *J. Phys. Chem. C* **2008**, *112*, 2654–2659; c) M. D. Halls, H. B. Schlegel, *J. Phys. Chem. B* **2002**, *106*, 1921–1925.
[3] L.-J. Li, A. N. Khlobystov, J. G. Wiltshire, G. A. D. Briggs, R. J. Nicholas, *Nat. Mater.* **2005**, *4*, 481–485.
[4] D. Obergfell, J. C. Meyer, M. Haluska, A. N. Khlobystov, S. Yang, L. Fan, D. Liu, S. Roth, *Phys. Status Solidi B* **2006**, *243*, 3430–3434.
[5] M. Ashino, D. Obergfell, M. Haluska, S. Yang, A. N. Khlobystov, S. Roth, R. Weisendanger, *Nat. Nanotechnol.* **2008**, *3*, 337–341.
[6] H. Ulbricht, T. Hertel, *J. Phys. Chem. B* **2003**, *107*, 14185–14190.
[7] A. N. Khlobystov, K. Porfyrakis, M. Kanai, D. A. Britz, A. Ardavan, T. J. S. Dennis, G. A. D. Briggs, *Angew. Chem.* **2004**, *116*, 1410–1413; *Angew. Chem. Int. Ed.* **2004**, *43*, 1386–1389.
[8] A. Chuvilin, A. N. Khlobystov, D. Obergfell, M. Haluska, S. Yang, S. Roth, U. Kaiser, *Angew. Chem.* **2010**, *122*, 197–201; *Angew. Chem. Int. Ed.* **2010**, *49*, 193–196.
[9] J. H. Warner, Y. Ito, M. H. Rummeli, T. Gemming, B. Buchner, H. Shinohara, G. A. D. Briggs, *Phys. Rev. Lett.* **2009**, *102*, No. 195504/1–4.
[10] Y. Sato, K. Suenaga, S. Okubo, T. Okazaki, S. Iijima, *Nano Lett.* **2007**, *7*, 3704–3708.
[11] H. Shinohara, *Rep. Prog. Phys.* **2000**, *63*, 843–892.
[12] R. Kitaura, N. Imazu, K. Kobayashi, H. Shinohara, *Nano Lett.* **2008**, *8*, 693–699.
[13] L. Guan, K. Suenaga, S. Okubo, T. Okazaki, S. Iijima, *J. Am. Chem. Soc.* **2008**, *130*, 2162–2163.
[14] J. T. Park, H. Song, J. J. Cho, M. K. Chung, J. H. Lee, I. H. Suh, *Organometallics* **1998**, *17*, 227–236.
[15] R. A. Sánchez-Delgado, M. Rosales, M. A. Esteruelas, L. A. Oro, *J. Mol. Catal. A* **1995**, *96*, 231–243.
[16] M. W. Pohlkamp, G. Kotzyba, U. A. Böcker, M. H. Gerdes, K. H. Wachtmann, W. Jeitschko, *Z. Anorg. Allg. Chem.* **2001**, *627*, 341–348.
[17] T. W. Chamberlain, A. M. Popov, A. A. Knizhnik, G. E. Samoilov, A. N. Khlobystov, *ASC Nano* **2010**, *4*, 5203–5210.
[18] T. W. Chamberlain, A. Camenisch, N. R. Champness, G. A. D. Briggs, S. C. Benjamin, A. Ardavan, A. N. Khlobystov, *J. Am. Chem. Soc.* **2007**, *129*, 8609–8614.
[19] D. A. Britz, A. N. Khlobystov, J. Wang, A. S. O'Neil, M. Poliakoff, A. Ardavan, G. A. D. Briggs, *Chem. Commun.* **2004**, 176–177.
[20] T. W. Chamberlain, R. Pfeiffer, H. Peterlik, H. Kuzmany, F. Zerbetto, M. Melle-Franco, L. Staddon, N. R. Champness, G. A. D. Briggs, A. N. Khlobystov, *Small* **2008**, *4*, 2262–2270.
[21] A. N. Khlobystov, D. A. Britz, A. S. O'Neil, J. Wang, M. Poliakoff, G. A. D. Briggs, *J. Mater. Chem.* **2004**, *14*, 2852–2857.
[22] T. Okazaki, K. Suenaga, K. Hirahara, S. Bandow, S. Iijima, H. Shinohara, *Physica B+C* **2002**, *323*, 97–99.
[23] T. Okazaki, K. Suenaga, K. Hirahara, S. Bandow, S. Iijima, H. Shinohara, *J. Am. Chem. Soc.* **2001**, *123*, 9673–9674.
[24] T. Shimada, Y. Ohno, K. Suenaga, T. Okazaki, S. Kishimoto, T. Mizutani, R. Taniguchi, H. Kato, B. Co, T. Sugai, H. Shinohara, *Jpn. J. Appl. Phys.* **2005**, *44*, 469–472.
[25] D. A. Britz, A. N. Khlobystov, *Chem. Soc. Rev.* **2006**, *35*, 637–659.
[26] A. V. Usatov, E. V. Martynova, I. S. Neretin, Y. L. Slovokhotov, A. S. Peregudov, Y. N. Novikov, *Eur. J. Inorg. Chem.* **2003**, 2041–2044.
[27] B. J. Huber, A. J. Poë, *Inorg. Chim. Acta* **1994**, *227*, 215–221.

Received: May 12, 2010
Published online: November 9, 2010

